Theoretical study of the central depression of nuclear charge density distribution by electron scattering*

LIU Jian(刘健)[1;1)] CHU Yan-Yun(褚衍运)[1]
REN Zhong-Zhou(任中洲)[1,2] WANG Zai-Jun(王再军)[3]

[1] Department of Physics, Nanjing University, Nanjing 210008, China
[2] Center of Theoretical Nuclear Physics, National Laboratory of Heavy-Ion Accelerator, Lanzhou 730000, China
[3] Department of Mathematics, Physics and Information Science, Tianjin University of Technology and Education, Tianjin 300222, China

Abstract: The charge form factors of elastic electron scattering for isotones with $N = 20$ and $N = 28$ are calculated using the phase-shift analysis method, with corresponding charge density distributions from relativistic mean-field theory. The results show that there are sharp variations at the inner parts of charge distributions with the proton number decreasing. The corresponding charge form factors are divided into two groups because of the unique properties of the s-states wave functions, though the proton numbers change uniformly in two isotonic chains. Meanwhile, the shift regularities of the minima are also discussed, and we give a clear relation between the minima of the charge form factors and the corresponding charge radii. This relation is caused by the diffraction effect of the electron. Under this conclusion, we calculate the charge density distributions and the charge form factors of the $A = 44$ nuclei chain. The results are also useful for studying the central depression in light exotic nuclei.

Key words: elastic electron scattering, RMF model, phase-shift analysis, central depression

PACS: 21.10.Ft, 25.30.Bf, 27.40.+z **DOI:** 10.1088/1674-1137/36/1/008

1 Introduction

High-energy electron scattering is a precise tool for probing nuclear structure, in particular nuclear charge densities [1, 2]. There are many advantages to elastic electron-nucleus scattering because the electromagnetic interaction between them is clearly understood and the nuclear properties are not influenced because the electron is a lepton. In the past few decades there have been many studies in this field and valuable and precise data have been obtained on nuclear electromagnetic properties [3–5]. However, owing to the limitation of making nucleus targets, electron scattering experiments were mainly carried out in past for stable nuclei [6–8]. In order to get the precise nuclear properties of exotic nuclei, elastic electron scattering experiments will be carried out in the near future at RIKEN and GSI [9–14]. So it is necessary for us to study the electron scattering of exotic nuclei theoretically in order to provide useful instructions for future experiments [15–22].

Nuclear matter (proton and neutron) distributions are the basic properties of nuclei. In the liquid drop model, nuclear charge distributions are regarded as a rigid sphere with saturated central charge densities and some modifications at its surface, approximately. With more and more electron scattering experiments being carried out, it has been found that there are central depressions in many nuclear charge distributions, which can be described by the three-parameter Fermi (3pF) model [23]. The ω parameter in the 3pF model is adjustable to illustrate how the central density is depressed [24]. In some exotic nuclei, as an extreme case of center-depressed nuclear

Received 6 April 2011
* Supported by National Natural Science Foundation of China (10775068,10735010,10975072,11035001), 973 National Major State Basic Research and Development of China (2007CB815004, 2010CB327803), CAS Knowledge Innovation Project (KJCX2-SW-N02) and Research Fund of Doctoral Point (RFDP) (20070284016, 20100091110028)
1) E-mail: liujian.nju@gmail.com

density, the nuclear bubble has attracted great attention. The concept of bubble nuclei was first studied by Wilson in 1946 [25] in order to explain equally spaced nuclear levels. From then on, many models have been used to investigate this phenomenon, such as the liquid-drop model, the Thomas-Fermi model and the Hartree-Fock-Bogoliubov method [26–28].

Though many different nuclear models have been used to interpret the central depression, the qualitative explanations for this phenomenon are similar. Because the s-states wave functions are the only ones with a non-zero value at $r = 0$, the lack of s-state nucleons will lead to a depletion of the density in the center of nucleus. In the nuclei near the stability line, the energy level of proton $2s_{1/2}$ lies between those of the $1d_{5/2}$ and $1d_{3/2}$ states. However, with the proton number decreasing, the spacing of the energy levels will be changed. It has been shown in many calculations that the $2s_{1/2}$ and $1d_{3/2}$ energy levels will inverse [29–31], and this is the main reason for the formation of the central depression in the s-d region.

As we know, electron-nucleus scattering is a precise tool to investigate nuclear charge distributions from stable to exotic ones. In the past few decades, much theoretical work has been devoted to the central depression phenomena of exotic isotones, but few calculations have been done on the corresponding electron scattering studies of these nuclei. In this article, we will discuss how the charge densities and charge form factors change along the $N = 20$, $N = 28$ and $A = 44$ nuclei with the proton number gradually decreasing. The charge distributions of these nuclei will be calculated by relativistic mean field (RMF) theory. Then the corresponding form factors of these nuclei will be investigated by the phase-shift analysis method. In the near future, the form factors could be determined through elastic electron scattering experiments. The results can be useful for future experiments and will also provide new tests of RMF theory for the unstable nuclei.

2 Theory

RMF theory has been very successful in describing nuclear properties. In this article, we calculate the wave functions of nucleons with the following effective Lagrangian [32–35].

$$\begin{aligned}\mathcal{L} = {} & \bar{\Psi}(\mathrm{i}\gamma^{\mu}\partial\mu - M)\Psi - g_{\sigma}\bar{\Psi}\sigma\Psi - g_{\omega}\bar{\Psi}\gamma^{\mu}\omega_{\mu}\Psi \\ & - g_{\rho}\bar{\Psi}\gamma^{\mu}\rho^{a}_{\mu}\tau^{a}\Psi - \frac{1}{2}m^{2}_{\sigma}\sigma^{2} - \frac{1}{3}g_{2}\sigma^{3} - \frac{1}{4}g_{3}\sigma^{4} \\ & - \frac{1}{4}\Omega^{\mu\nu}\Omega_{\mu\nu} + \frac{1}{2}m^{2}_{\omega}\omega^{\mu}\omega_{\mu} - \frac{1}{4}\vec{R}^{\mu\nu}\cdot\vec{R}_{\mu\nu} \\ & + \frac{1}{2}m^{2}_{\rho}\vec{\rho}^{\mu}\cdot\vec{\rho}_{\mu} - \frac{1}{4}F^{\mu\nu}F_{\mu\nu} \\ & - \mathrm{e}\bar{\Psi}\gamma^{\mu}A_{\mu}\frac{1}{2}(1-\tau^{3})\Psi, \end{aligned} \tag{1}$$

with the tensor field

$$\Omega^{\mu\nu} = \partial^{\mu}\omega^{\nu} - \partial^{\nu}\omega^{\mu}, \tag{2}$$

$$\vec{R}^{\mu\nu} = \partial^{\mu}\vec{\rho}^{\nu} - \partial^{\nu}\vec{\rho}^{\mu}, \tag{3}$$

$$F^{\mu\nu} = \partial^{\mu}A^{\nu} - \partial^{\nu}A^{\mu}, \tag{4}$$

Based on the no-sea approximation and the mean-field approximation, the motion equations can be solved iteratively with this Lagrangian. Then the nuclear charge distribution can be obtained. The charge density distribution is assumed to be contributed entirely by the protons, and can be obtained in the following way

$$\rho_{\mathrm{c}}(\boldsymbol{r}) = \int \rho_{\mathrm{p}}(\boldsymbol{r}')\rho^{\mathrm{p}}(\boldsymbol{r}-\boldsymbol{r}')\mathrm{d}\boldsymbol{r}', \tag{5}$$

where $\rho^{\mathrm{p}}(\boldsymbol{r})$ is the single proton charge distribution.

With the nuclear charge density obtained, the electro-static potential between the electron and nucleus can be determined as follows:

$$V_{\mathrm{c}}(\boldsymbol{r}) = -\frac{e^{2}}{4\pi\epsilon_{0}}\int\frac{\rho_{\mathrm{c}}(\boldsymbol{r}')}{|\boldsymbol{r}-\boldsymbol{r}'|}\mathrm{d}\boldsymbol{r}'. \tag{6}$$

Once the $V_c(\boldsymbol{r})$, which is used to describe the interaction between the electron and nucleus is known, the Dirac equation

$$[\alpha\cdot\boldsymbol{p} + \beta m + V(\boldsymbol{r})]\Psi(\boldsymbol{r}) = E\Psi(\boldsymbol{r}), \tag{7}$$

can be decomposed into different partial waves with definite orbital angular momentum and spin orientation. The phase shifts, which are characterized into spin-up ones δ_l^+ and spin-down ones δ_l^-, can be worked out by solving the Dirac equation with a scattering boundary condition [36]. Then we can calculate the elastic electron-nucleus scattering cross section by:

$$\frac{\mathrm{d}\sigma}{\mathrm{d}\Omega} = |f(\theta)|^{2} + |g(\theta)|^{2}, \tag{8}$$

with

$$f(\theta) = \frac{1}{2\mathrm{i}k}\sum_{l=0}^{\infty}[(l+1)(\mathrm{e}^{2\mathrm{i}\delta_{l}^{+}}-1) - l(\mathrm{e}^{2\mathrm{i}\delta_{l}^{-}}-1)]P_{l}(\cos\theta), \tag{9}$$

and

$$g(\theta) = \frac{1}{2\mathrm{i}k}\sum_{l=0}^{\infty}[\mathrm{e}^{2\mathrm{i}\delta_{l}^{+}} - \mathrm{e}^{2\mathrm{i}\delta_{l}^{-}}]P_{l}^{1}(\cos\theta), \tag{10}$$

in which P_l and P_l^1 are the Legendre function and associated Legendre function, respectively.

The charge form factor is defined as

$$|F(q)|^2 = \frac{\mathrm{d}\sigma/\mathrm{d}\Omega}{\mathrm{d}\sigma_{\mathrm{M}}/\mathrm{d}\Omega}, \tag{11}$$

where $\mathrm{d}\sigma_{\mathrm{M}}/\mathrm{d}\Omega$ denotes the Mott cross section and q denotes the transferred momentum.

3 Numerical results and discussion

In this section we present the numerical results of the charge density distributions from the RMF model, and the charge form factors from the phase-shift analysis method for the nuclei ^{34}Si, ^{36}S, ^{38}Ar, ^{40}Ca, ^{42}Ti and ^{44}Cr with neutron number $N = 20$; nuclei ^{42}Si, ^{44}S, ^{46}Ar, ^{48}Ca, ^{50}Ti and ^{52}Cr with neutron number $N = 28$, and ^{44}Si, ^{44}S, ^{44}Ar, ^{44}Ca, ^{44}Ti and ^{44}Cr with nucleon number $A = 44$. A detailed discussion will also be given with these results.

To begin with, we give the root-mean-square (rms) charge radii and binding energies per nucleon for the considered nuclei in Table 1, which are calculated in the RMF model with the NL-SH force parameter set. During the calculation, the pairing interactions are taken into consideration by the BCS treatment, and the pairing gaps are chosen to be $\Delta_{\mathrm{n}} = \Delta_{\mathrm{p}} = 11.2/\sqrt{A}$ MeV. It can be seen in Table 1 that the theoretical rms charge radii and binding energies coincide with the experimental ones well. So we can conclude that RMF theory is reliable in predicting the nuclear properties for both the stable and exotic ones.

Table 1. The rms charge radii (fm) and binding energies per nucleon (MeV) for the $N = 20$, $N = 28$ and $A = 44$ nuclei. The theoretical ones are calculated from the RMF model with the NL-SH parameter set. The experimental data are taken from Ref. [37, 38].

	nuclei	R_{c}	R_{c}(Expt.)	B	B(Expt.)
$N=20$	^{34}Si	3.217		8.346	8.336
	^{36}S	3.347	3.298	8.520	8.575
	^{38}Ar	3.448	3.402	8.570	8.614
	^{40}Ca	3.568	3.476	8.539	8.551
	^{42}Ti	3.745		8.276	8.269
	^{44}Cr	3.870		7.969	7.951
$N=28$	^{42}Si	3.224		7.413	7.372
	^{44}S	3.323		7.984	7.994
	^{46}Ar	3.400	3.436	8.397	8.411
	^{48}Ca	3.472	3.474	8.668	8.666
	^{50}Ti	3.545	3.570	8.742	8.756
	^{52}Cr	3.611	3.642	8.753	8.775
$A=44$	^{44}Si	3.232		7.049	7.076
	^{44}S	3.324		7.981	7.994
	^{44}Ar	3.388		8.487	8.493
	^{44}Ca	3.459	3.515	8.668	8.658
	^{44}Ti	3.539		8.461	8.553
	^{44}Cr	3.622		7.950	7.951

3.1 The isotonic chains with $N = 20$ and $N = 28$

The charge density distributions for the $N = 20$ and $N = 28$ isotonic nuclei are presented in Figs. 1 and 2, which are calculated using the NL-SH force parameter set. It can be seen from Fig. 1 that the variation in the charge density distributions can be roughly divided into two groups. One group includes ^{40}Ca, ^{42}Ti and ^{44}Cr, and the other consists of ^{34}Si, ^{36}S and ^{38}Ar. In the first group there are obvious peaks at the center of their charge distributions. For the second group the charge distributions are quite different and instead of the central peaks there are central depressions for all these nuclei, and the central nuclear charge densities are more depressed when the nuclei become more proton-deficit.

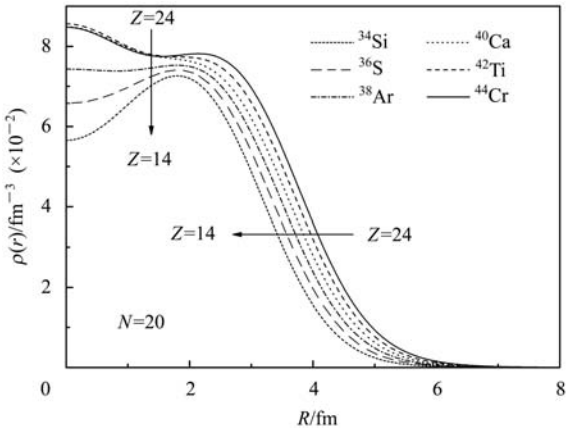

Fig. 1. Variations of charge density distributions for the $N = 20$ (Z=14–24) isotonic nuclei calculated with the RMF model.

This variation is caused by the inversion of the proton $2s_{1/2}$ and $1d_{3/2}$ states with the proton number decreasing. From the consequences of RMF theory, the energy of the $2s_{1/2}$ proton states is a little higher than the $1d_{3/2}$ states in the considered $N = 20$ nuclei. The energy difference of the two states is quite small and both of them are much higher than the $1d_{5/2}$ state. When $Z = 14$, the $1d_{5/2}$ state is fully filled and the $1d_{3/2}$ and $2s_{1/2}$ states are almost empty, which causes the central charge density of ^{34}Si to be more depressed. But when the proton number increases, the probability for the new added proton to

occupy the $1d_{3/2}$ state or the $2s_{1/2}$ state is almost the same because the two proton energy states are close enough. So the number of protons in the $1d_{3/2}$ and $2s_{1/2}$ state grows simultaneously with the proton number increasing, which leads to the gradual increase in the central charge densities in ^{34}Si, ^{36}S and ^{38}Ar. When the proton number is 20 or more than 20, the $2s_{1/2}$ states are fully filled, which leads to the central peaks in ^{40}Ca, ^{42}Ti and ^{44}Cr.

Figure 2 shows the charge density distributions for the $N = 28$ isotonic nuclei. It can be clearly seen that these nuclear charge density distributions can also be divided into two groups. The nuclei ^{48}Ca, ^{50}Ti and ^{52}Cr make up one group, which has central peaks, and ^{42}Si, ^{44}S and ^{46}Ar make up the other one, which has obvious central depressions. Compared to the isotonic nuclei with $N = 20$, the charge density distributions for the $N = 28$ isotonic chain have a more rapid vibration at the center. The effect also results from the inversion of the proton $2s_{1/2}$ and $1d_{3/2}$ states in the isotones with $N = 28$. However, unlike the situation in the $N = 20$ nuclei, the energies of the $2s_{1/2}$ states are higher than the $1d_{3/2}$ states in the $N = 28$ nuclei. When $Z = 14$, the $1d_{5/2}$ state is fully filled, and the $1d_{3/2}$ and $2s_{1/2}$ states are almost empty. With the proton number increasing, the probabilities for new added protons to occupy the $1d_{3/2}$ state are much higher than the $2s_{1/2}$ state because the energy of the $1d_{3/2}$ state is lower enough than that of the $2s_{1/2}$ state. During the process, the $2s_{1/2}$ states are almost empty, which leads to serious central depressions of charge distributions in ^{42}Si, ^{44}S and ^{46}Ar. When the proton number comes to 18, the $1d_{3/2}$ state is fully filled, and the new protons will all occupy the $2s_{1/2}$ state if the proton number increases continually. The sharp increase in the proton number of the $2s_{1/2}$ state will lead to a sharp increase in the central charge densities in the considered nuclei.

Taking the charge density distributions in Fig. 1 and Fig. 2 as inputs, the corresponding charge form factors are further calculated with the phase-shift analysis method. The variations in the form factors with the proton number changing can be studied. The charge form factors for the $N = 20$ isotopic chains are presented in Fig. 3. It can be seen from Fig. 3 that the charge form factors have inward and upward shifts as the proton number increases. The charge form factors in the moderate momentum transfer can also be divided into two groups. The first group includes ^{40}Ca, ^{42}Ti and ^{44}Cr, and the spacings between their moment transfers of the second minimum are 0.05 fm^{-1}. The nuclei ^{34}Si, ^{36}S and ^{38}Ar make up the second group, and the spacings between their momentum transfers of the second minimum are 0.11 fm^{-1}. We discussed that the charge density distributions are divided into two groups in Fig. 1. The variations in charge form factors are the same as the variations in the corresponding charge densities of these nuclei. This also indicates that electron nucleus scattering is a precise tool that can be used to probe nuclear charge densities.

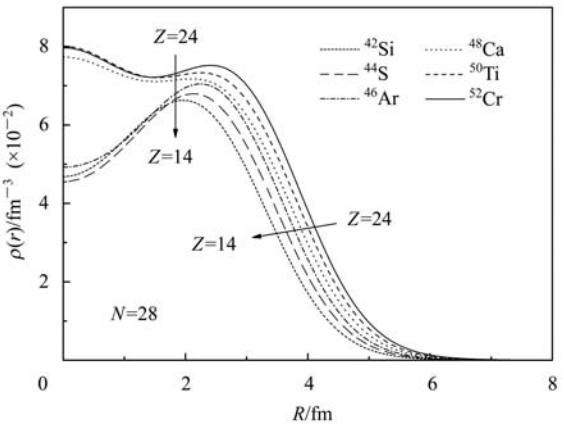

Fig. 2. Variations in charge density distributions for the $N = 28$ (Z=14–24) isotonic nuclei calculated with the RMF model.

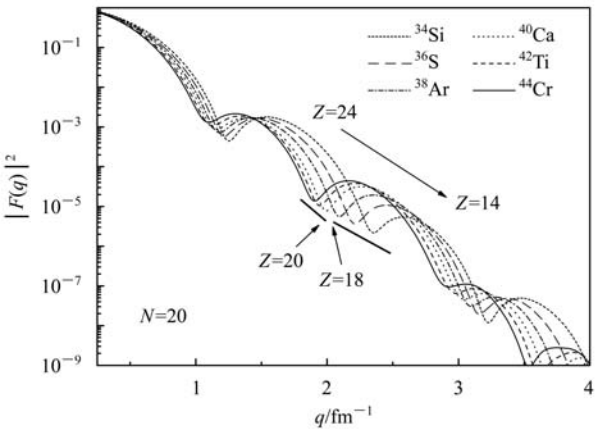

Fig. 3. Variations in the charge form factor with the proton number for $N = 20$ (Z=14–24) isotonic nuclei.

In Fig. 4, we present the variation in charge form factors for the $N = 28$ isotonic nuclei. It can also be seen clearly in Fig. 4 that the form factors of these nuclei can be divided into two groups in the moderate momentum transfer. The nuclei ^{48}Ca, ^{50}Ti and ^{52}Cr make up one group whose spacings between their momentum transfers of the second minima are 0.05 fm^{-1}.

The nuclei ^{34}Si, ^{36}S and ^{38}Ar make up the other one, whose spacings between their momentum transfers of the second minima are 0.12 fm^{-1}. The considered nuclei are grouped into two same types in Fig. 4, just as in the corresponding charge density distributions in Fig. 2. Meanwhile, compared to Fig. 3, the spacing of the two groups in Fig. 4 is much larger. This is because the corresponding charge densities change sharply at the center in the $N = 28$ isotones but change gradually at the center in the $N = 20$ isotones.

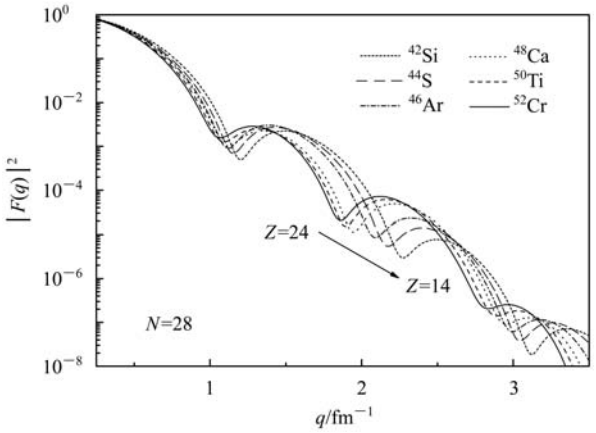

Fig. 4. Variations in the charge form factor with the proton number for $N = 28$ (Z=14–24) isotonic nuclei.

In the present work, the theoretical charge form factors are obtained using the RMF model with the NL-SH parameter set. Calculations with other parameter sets such as NL3 and TM2 are similar to the results in Figs. 3 and 4. But if we take a different nuclear model such as the large-scale shell-model, there will be a different description of the charge distribution, and the corresponding charge form factor will also be different. As we know, elastic electron scattering is a precise tool to detect charge distributions, so it can help us to check the validity of the models and constrain their parameters. The results in the present work can provide future experiments with some useful instructions in advance, and meanwhile the future experiments will help us to check and constrain the parameters of the RMF model.

3.2 The hard-sphere model nuclei and the nuclei chain with $A = 44$

It has been shown in many studies [19, 20, 22] that the minima of charge form factors shift inwards and upwards with the charge numbers and charge radii of the target nuclei changing. The regularities of the shifts of the minima will be studied in the following. First, the regularities of the charge form factors will be studied, whose corresponding charge density distributions are described in the hard-sphere model. Then we will analyze the scattering charge form factors, whose corresponding charge densities are calculated in the RMF model. During these calculations we use the $A = 44$ nuclei chains as the considered nuclei.

The charge form factors of the hard-sphere model are presented in Fig. 5, and the momentum transfers of the minima can be found in this graph. We can see that the positions of the minima are not sensitive to the charge numbers but very sensitive to the charge radii, which are caused by the diffraction effect of the electron. It can also be found in Fig. 5 that the shapes and magnitudes of the form factors depend on the charge numbers rather than the charge radii. When the charge radii change, the positions of the form factors shift inwards, however the magnitudes do not change.

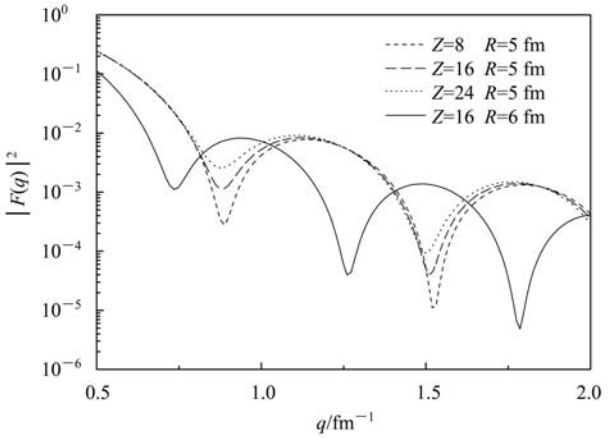

Fig. 5. Variations in the charge form factors with charge number and charge radius. The corresponding charge density distributions are represented by the sphere-hard model, and the charge form factors are calculated with the phase-shift method. The charge number chooses Z =8, 16, 24, respectively, and the charge radii choose $R = 5$ fm and $R = 6$ fm, respectively.

Because the RMF model is more accurate in describing nuclear charge distributions, in the following part we will discuss this problem in the RMF model. We choose the nuclei ^{44}Si, ^{44}S, ^{44}Ar, ^{44}Ca, ^{44}Ti and ^{44}Cr with the mass number $A = 44$ as the considered nuclei. They have the same mass number so will have equal charge radii if they are described in the hard-sphere model. From the analysis of these nuclei, we can see the limitation of the hard-sphere model in describing the nucleus. Meanwhile, the proton numbers

of these nuclei cross the $2s_{1/2}$ and $1d_{3/2}$ states and a similar regularity of central depression will be given, as in the discussed situation about the $N = 20$ and $N = 28$ isotonic chains.

The charge density distributions of the $A = 44$ nuclei are presented in Fig. 6. It can be seen from Fig. 6 that the charge densities can also be divided into two groups. One group includes the ^{44}Ca, ^{44}Ti and ^{44}Cr nuclei, which have central peaks in their charge distributions, and the other includes the ^{44}Si, ^{44}S and ^{44}Ar nuclei, which have central depressions. The reason for this is similar to that discussed for the $N = 28$ isotonic chain. The effect also results from the inversion of the proton $2s_{1/2}$ and $1d_{3/2}$ states in the considered nuclei. The energy of the $2s_{1/2}$ states is higher than the $1d_{3/2}$ states, and the new added protons prefer to occupy the $1d_{3/2}$ states. At the beginning, the nuclei are lacking the s-state protons. However, when the $1d_{3/2}$ state is fully filled, there will be a sharp increase in the number of s-state protons, so the central charge density will also change rapidly from a central depression to a central peak.

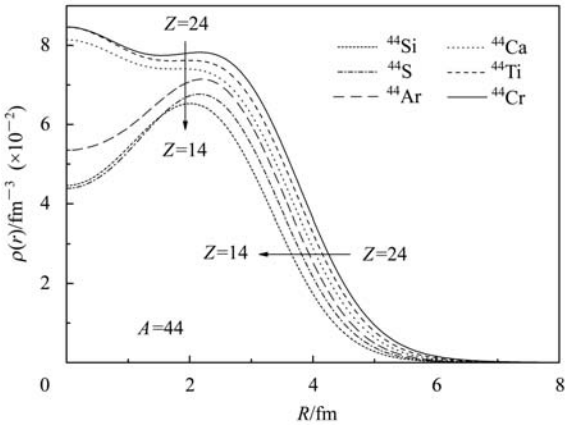

Fig. 6. Variations in charge density distributions for the $A = 44$ (Z=14–24) isotonic nuclei calculated with the RMF model.

Taking the charge density distributions in Fig. 6 as inputs, the corresponding charge form factors are calculated and presented in Fig. 7. We can also divide the charge form factors into two groups, the ^{44}Ca, ^{44}Ti and ^{44}Cr nuclei for one group, and the ^{44}Si, ^{44}S and ^{44}Ar nuclei for the other. In the first group, their second minimum positions are almost the same and only the magnitudes of the second minimum factors are different. This situation is similar to the result of the hard-sphere model. In the second group, the minima are not at the same position. Both of these nuclei groups have the same mass number, so their charge radii should be the same if considered in the hard-sphere model because nuclear radii are in proportion to $A^{1/3}$ in the hard-sphere model. The minima positions will also be the same as shown in Fig. 5. However, it can be found in Fig. 7 that their minima do not coincide with each other and can be divided into two groups in the moderate momentum transfer in the RMF model. If similar experimental data could be obtained in the future, it will again prove that the hard-sphere model is too crude to describe nuclear charge distribution.

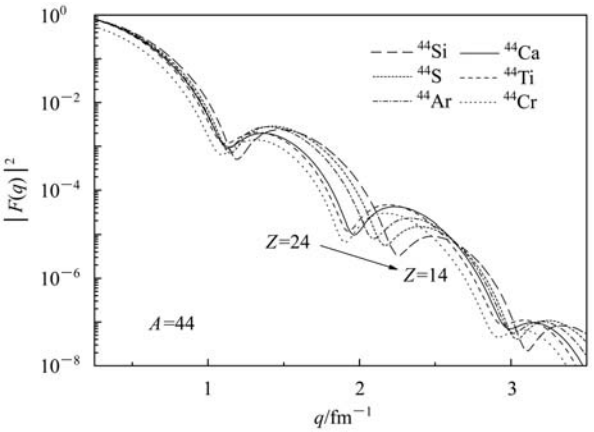

Fig. 7. Variations in charge form factor with the proton number for the $A = 44$ (Z=14–24) nuclei calculated with the RMF method.

4 Summary

In summary, the charge density distributions and charge form factors for $N = 20$ and $N = 28$ isotonic nuclei have been calculated. The variations in the charge distributions and charge form factors are investigated. It was found that the charge distributions of $N = 20$ and $N = 28$ isotones have different variations at the center because of the different energy level spacings of the proton states in two chains. The charge distributions of the two isotonic chains can be divided into two groups. One group has central peaks and the other has central depressions. These effects are caused by the inversion of the $2s_{1/2}$ and $1d_{3/2}$ states in the considered nuclei. The variations in central charge densities for $N = 28$ nuclei are more rapid than those for $N = 20$ nuclei. This is because the energy of the $2s_{1/2}$ proton state is much higher than the $1d_{3/2}$ state in $N = 28$ isotones, but in $N = 20$ nuclei the energy of the two levels is almost equal. The new protons are more likely to occupy the $1d_{3/2}$ state in $N = 28$ isotones, so this leads to a sharp increase in the number of s-state protons in the $N = 28$ isotones, but in the $N = 20$ isotonic chains the number of s-state protons increases gradually.

It is well known that the elastic electron-nucleus scattering form factor is directly related to its charge density distribution. So variations in charge density distributions will lead to similar variations in the corresponding charge form factors. From Figs. 3 and 4, we can find that the charge form factors in the moderate momentum transfer are also divided into two groups, and this coincides with the conclusion that the form factors in the moderate and high momentum transfers are sensitive to the inner parts of the charge density distributions. So the results obtained in this paper can be used as references for future experiments to explore nuclear central depression in exotic nuclei. Meanwhile, future experiments will also help us to check the model and constrain the parameters.

Finally we discuss the shift of charge form factors with the charge number and charge radius changing in the hard-sphere model. From the results we find that the minima positions are not sensitive to the charge numbers but very sensitive to the charge radii. However, the magnitudes of the form factors depend on the charge numbers rather than the charge radii. Under this conclusion we calculate the charge density distributions and charge form factors of the $A = 44$ nuclei chain, which should have the same nuclear radii if described in the hard-sphere model. However, from the calculation with the RMF method, it can be found in Fig. 6 that the charge densities of these nuclei can also be divided into two groups, just like the isotones with $N = 20$ and $N = 28$. The corresponding charge form factors in Fig. 7 show that their first minima positions are almost the same, which coincides with the conclusion of the hard-sphere model. But in the moderate momentum transfer they divide into two groups, which reflect the details of the inner parts of the charge density distributions. If similar experimental data can be obtained in the future, it will again prove that the hard-sphere model is too crude to describe nuclear charge distribution. Meanwhile, the results can also be used as a reference for future experiments to probe the central depression in exotic nuclei.

References

1 Donnelly T W, Walecka J D. Annu. Rev. Nucl. Part. Sci., 1975, **25**: 329
2 Donnelly T W, Sick I. Rev. Mod. Phys., 1984, **56**: 461
3 Hofstadter R. Rev. Mod. Phys., 1956, **28**:214
4 de Vries H, de Jager C W. At. Data Nucl. Data Tables, 1987, **36**: 495
5 Fricke G, Bernhardt C, Heiling K et al. At. Data Nucl. Data Tables, 1995, **60**: 177
6 Litvinenko A S, Shevchenko N G, Buki A Yu et al. Nucl. Phys. A, 1972, **182**: 256
7 Friar J L, Negele J W. Nucl. Phys. A, 1973, **212**: 93
8 Sick I. Nucl. Phys. A, 1974, **218**: 509
9 Sick I. Prog. Part. Nucl. Phys., 2001, **47**: 245
10 Suda T, Wakasugi M. Prog. Part. Nucl. Phys., 2005, **55**: 417
11 Simon H. Nucl. Phys. A, 2007, **787**: 102
12 An International Accelerator Facility for Beams of Ions and Antiprotons, GSI Report, 2006 (unpublished) [http://www.gsi.de/GSI-Future/cdr/]
13 Wakasugi et al. Phys. Rev. Lett., 2008, **100**: 164801
14 Suda T et al. Phys. Rev. Lett., 2009, **102**: 102501
15 Antonov A N, Kadrev D N, Gaidarov M K et al. Phys. Rev. C, 2005, **72**: 044307
16 Roca-Maza X, Centelles M, Salvat F et al. Phys. Rev. C, 2008, **78**: 044332
17 Karataglidis S, Amos K. Phys. Lett. B, 2005, **650**: 148
18 Bertulani C A. Phys. Lett. B, 2005, **624**: 203
19 WANG Z, REN Z. Phys. Rev. C, 2004, **70**: 034303
20 WANG Z, REN Z. Nucl. Phys. A, 2007, **749**: 47
21 DONG T, REN Z, GUO Y. Phys. Rev. C, 2007, **76**: 054602
22 CHU Y, REN Z, DONG T et al. Phys. Rev. C, 2009, **79**: 044313
23 de Jager C W, de Vries H, de Vries C. At. Data Nucl. Data Tables, 1974, **14**: 479
24 CHU Y, REN Z, WANG Z. Phys. Rev. C, 2010, **82**: 024302
25 Wilson H A. Phys. Rev., 1946, **69**: 538
26 Siemens P, Bethe H A. Phys. Rev. Lett., 1967, **18**: 704
27 Swiatecki W J. Phys. Scr., 1983, **28**: 349
28 Decharge J, Berger J F, Grirod M et al. Nucl. Phys. A, 2003, **716**: 55
29 Todd-Rudel B G, Piekarewicz J, Cottle P D. Phys. Rev. C, 2004, **69**: 021301
30 Grasso M, Gauderfroy L, Khan E et al. Phys. Rev. C, 2009, **79**: 034318
31 Khan E, Grasso M, Margueron J et al. Nucl. Phys. A, 2008, **800**: 37
32 Horowitz C J, Serot B D. Nucl. Phys. A, 1981, **368**: 503
33 Reinhard P G. Rep. Prog. Phys., 1989, **52**: 439
34 REN Z, Facessler A, Bobyk A. Phys. Rev. C, 1998, **57**: 2752
35 Ring P. Prog. Part. Nucl. Phys., 1996, **37**: 193
36 Salvat F, Jabalonski A, Powell C J. Comput. Phys. Commun., 2005, **165**: 157
37 Angeli I. At. Data Nucl. Data Tables, 2004, **87**: 185.
38 Audi G, Wapstra A H, Thibault C. Nucl. Phys. A, 2003, **729**: 337